



HAL
open science

Phosphorus removal from wastewater by carbonated bauxite residue under aerobic and anoxic conditions

Cristian Barca, Dario Scanu, Nicola Podda, Helene Miche, Laurent Poizat,
Pierre Hennebert

► To cite this version:

Cristian Barca, Dario Scanu, Nicola Podda, Helene Miche, Laurent Poizat, et al.. Phosphorus removal from wastewater by carbonated bauxite residue under aerobic and anoxic conditions. *Journal of Water Process Engineering*, 2021, pp.101757. 10.1016/j.jwpe.2020.101757 . hal-03036764

HAL Id: hal-03036764

<https://hal.science/hal-03036764v1>

Submitted on 2 Dec 2020

HAL is a multi-disciplinary open access archive for the deposit and dissemination of scientific research documents, whether they are published or not. The documents may come from teaching and research institutions in France or abroad, or from public or private research centers.

L'archive ouverte pluridisciplinaire **HAL**, est destinée au dépôt et à la diffusion de documents scientifiques de niveau recherche, publiés ou non, émanant des établissements d'enseignement et de recherche français ou étrangers, des laboratoires publics ou privés.



Distributed under a Creative Commons Attribution - NonCommercial - NoDerivatives 4.0
International License

1 **Phosphorus removal from wastewater by carbonated bauxite residue under**
2 **aerobic and anoxic conditions**

3 Cristian Barca^{a,*}, Dario Scanu^{a,b}, Nicola Podda^{a,b}, H el ene Miche^c, Laurent Poizat^d, Pierre
4 Hennebert^e

5 ^a Aix-Marseille University, CNRS, Centrale Marseille, M2P2 UMR 7340, Marseille, France

6 ^b Department of Civil-Environmental Engineering and Architecture (DICAAR), University of
7 Cagliari, Via Marengo 2, 09123 Cagliari, Italy

8 ^c Aix-Marseille University, CNRS, IRD, INRAE, Coll ege de France, UM 34 CEREGE, Aix en
9 Provence, France

10 ^d ALTEO Gardanne, Route de Biver, BP 43, F-13541 Gardanne Cedex, France

11 ^e INERIS, BP 2, F-60550 Verneuil-en-Halatte, France

12 *corresponding author: cristian.barca@univ-amu.fr

13 **Abstract**

14 This study aimed at evaluating the potential use of carbonated bauxite residue (CBR) as filter
15 substrate to upgrade phosphorus (P) removal in small wastewater treatment plants such as
16 constructed wetlands. Comparative experiments of P removal were performed in two columns
17 continuously fed with synthetic and real wastewater to investigate the behavior of CBR under
18 aerobic (column A) and anoxic biotic conditions (column B). The effect of various parameters,
19 including pH, temperature, addition of organic carbon, and dissolved oxygen concentration,
20 was investigated. Also, a series of chemical extractions was performed to elucidate the main
21 mechanisms of P removal achieved by CBR. Over 140 days of operation, columns A and B
22 showed a total P removal performance of 98.5% and 91.6%, thus reaching a total P removal
23 capacity of 0.63 mg P/g CBR and 0.61 mg P/g CBR, respectively. The results indicate that

1 aeration conditions and microbial activity can significantly affect the performance of CBR
2 filters. Under aerobic conditions, precipitation of Ca-P complexes appears to be the main
3 mechanism leading to P removal. Under anoxic biotic conditions, microbially driven
4 mobilization of Fe from CBR may provide Fe ions for Fe-P precipitation, but also it may lead
5 to Fe release from the filters. This study provides crucial information to evaluate the potential
6 use of CBR at different steps of the wastewater treatment process. Overall, the results indicate
7 that the use of CBR filters is particularly suitable as a tertiary treatment step to remove P from
8 effluents with low organic load under aerobic conditions.

9 **Keywords:** wastewater treatment; phosphorus removal; bauxite residue; constructed wetland;
10 reactive filter.

11 **1 Introduction**

12 Nowadays, improving phosphorus (P) removal performances in small wastewater treatment
13 plants (WWTPs) such as constructed wetlands (CWs) represents a topical issue for researchers
14 and professionals in the field of wastewater treatment [1]. Several strategies are currently being
15 studied, including the enhanced P biological uptake by intermittent aeration [2], the use of
16 electrochemical methods to intensify electron exchanges [3], the improvement of iron dosing
17 strategies for efficient P removal [4], and the selection of wetland plants and substrate materials
18 with high P sorption capacities [5,6]. During the last decade, the use of separate filter units
19 filled with reactive materials having a high affinity for P binding has been proposed as a
20 promising solution to upgrade P removal performances in CWs [7–10]. A large variety of
21 reactive materials, including natural soils and sediments, industrial wastes and by-products, and
22 manufactured adsorbent materials, have been tested for P removal [11–13]. Most of these
23 materials present high contents of calcium (Ca), iron (Fe), and/or aluminum (Al), which are
24 elements with a strong affinity for P binding [13,14].

1 Several international studies have demonstrated that bauxite residue, a Fe and Al oxide-rich
2 waste from the aluminum industry, is an efficient filter material for P removal from wastewater
3 [15–18]. According to Evans [19], aluminum industry produces about 150 Mt per year of
4 bauxite residue worldwide, of which no more of 3-5% is reused in a productive way (*e.g.* cement
5 and ceramic production) [20]. This indicates a very interesting potential market of bauxite
6 residue valorization as filter substrate in CWs. Maximum P removal capacities ranged from 6
7 to up than 12 mg P/g bauxite residue [16,17], thus depending on the type and composition of
8 bauxite residue and on the experimental parameters established for the experiments. The main
9 mechanisms leading to P removal were anionic adsorption on functional sites (*e.g.* -OH) and
10 precipitation of Ca-P complexes on the mineral surface of bauxite residue [17]. Due to its high
11 alkaline nature [19], bauxite residue can produce high pH leachates (up to 13) [20], and
12 therefore a pretreatment with gypsum was efficiently proposed by Cusack *et al.* [15] to
13 neutralize its alkalinity and reduce pH leachates below 9. However, most of these studies were
14 performed in batch and using synthetic P solutions, which did not contain all the components
15 occurring in real effluents that may affect P removal performances (*e.g.* microorganisms and
16 organic compounds, competing ions, suspended solids). Moreover, results from batch
17 experiments usually cannot be directly employed to preview the behavior of field scale filters,
18 as treatment performances and P removal mechanisms can differ under dynamic operating
19 conditions. To the best of our knowledge, only a study in the literature has investigated P
20 removal performances of bauxite residue in small-scale columns continuously fed with real
21 effluents [21]. Furthermore, there is a lack of data in the literature concerning the effect of
22 aeration conditions and microbial activity on the performance of bauxite residue filters.

23 This study aimed at evaluating performances and determining P removal mechanisms of
24 carbonated bauxite residue (CBR) under aerobic and anoxic biotic conditions. Indeed, the
25 organic content in wastewater and/or the addition of external organic carbon to the effluents,

1 which is often used as a strategy to enhance heterotrophic denitrification in WWTPs [22,23],
2 may promote the establishment of anoxic biotic conditions in water saturated filters. Therefore,
3 knowledge and understanding of the effect of different aeration conditions and microbial
4 activity on the behavior of CBR are indispensable to evaluate its potential use as filter substrate
5 at different steps of the wastewater treatment process in CWs. The novelty and importance of
6 this paper are highlighted by the following two points:

7 (i) The first comparative investigation of P removal performances of CBR under aerobic and
8 anoxic conditions in dynamic flow experiments. Two laboratory scale columns were filled with
9 CBR and continuously fed with synthetic and real CW effluents. The effect of various
10 parameters, including pH, temperature, addition of organic carbon, and dissolved oxygen
11 concentration, on P removal performances was investigated.

12 (ii) An in-depth critical investigation of the P removal mechanisms achieved by CBR. A
13 systemic approach, which involves the integration and analysis of the experimental results of
14 water quality monitoring and chemical extractions from CBR, was followed to investigate
15 mineralogical changes and to elucidate the main mechanisms of P removal achieved by CBR
16 under aerobic and anoxic biotic conditions.

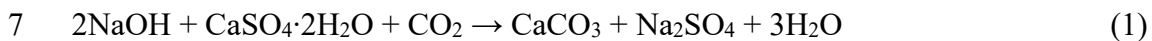
17 Overall, the results of this study allow evaluating the behavior of CBR under real operating
18 scenarios, and they provide crucial information for the scale up of the filters from the laboratory
19 to the field scale.

20 **2 Materials and methods**

21 **2.1 Bauxite residue collection and preparation**

22 The samples of bauxite residue used in this study were provided by the company ALTEO
23 (Gardanne, France). Their main chemical composition was Fe₂O₃ (45-53%), Al₂O₃ (10-16%),
24 TiO₂ (9-15%), SiO₂ (5-8%), CaO (3-8%), and Na₂O (3-5%) (data from ALTEO). Before

1 column experiments, bauxite residues were mixed with gypsum ($\text{CaSO}_4 \cdot 2\text{H}_2\text{O}$) at a dried mass
2 ratio of 5% (mass of gypsum to mass of bauxite residue) and put in contact with the atmosphere
3 to produce CBR. This was done to neutralize the NaOH content of bauxite residue by
4 carbonation and calcium carbonate precipitation, according to equation (1), and to decrease the
5 pH of CBR leachates below a value of 9 as described by Cusack *et al.* [15] and experienced in
6 large scale on the storage site of ALTEO.

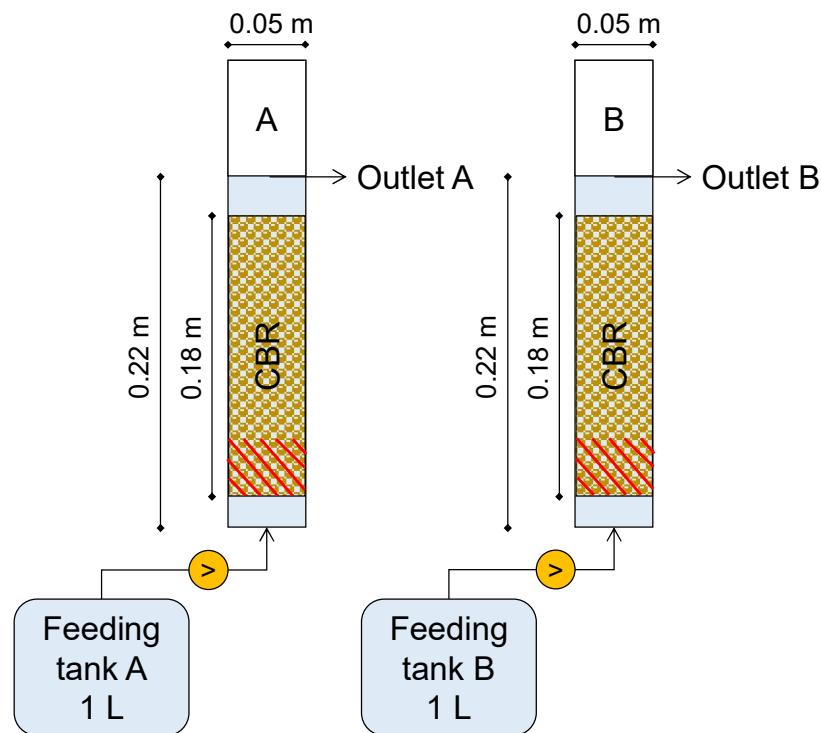


8 After carbonation, CBR was sieved and the fraction less than 2 mm was collected to perform
9 column experiments. CBR samples were dried at 45 °C overnight to reduce their water content
10 before the experiments. The temperature of 45 °C was selected in order to reduce the risk of
11 changes in the mineralogical composition during drying [24]. The remaining water content of
12 CBR was determined after heating at 105 °C until constant weight.

13 **2.2** *Set-up of column experiments*

14 Two glass columns of total volume 0.59 L were filled with about 0.35 L of CBR each, thus
15 corresponding to about 0.45 kg dried mass of CBR *per* column (columns A and B). The main
16 details of the column design are shown in Fig. 1. During the full period of operation, the
17 columns were continuously fed according to a vertical up-flow of about 12 mL/h, thus giving a
18 theoretical hydraulic retention time based on the initial void volume (HRT_v) of around 24 h.
19 During the first 54 days of operation, column A was fed with a synthetic solution of about 10
20 mg P/L and 40 mg N/L (prepared with tap water, KH_2PO_4 , and KNO_3). These P and nitrogen
21 (N) concentrations are in good agreement with the average outlet concentrations of vertical flow
22 CWs in France (total-P 8 ± 3 mg P/L, phosphate-P 8 ± 2 mg P/L, total Kjeldahl-N 7 ± 7 mg
23 N/L, ammonium-N 5 ± 6 mg N/L, and nitrate-N 56 ± 25 mg N/L, average values \pm standard
24 deviations of 151 plants) [25]. Then, from day 55 to 140, the column A was fed with the real

1 effluent of a vertical flow CW that treats the domestic wastewater of a small French
2 municipality (1500 people equivalent, Rougiers, France). During the same periods of operation,
3 the column B was operated identically to column A, but with the only difference that the feeding
4 solutions were enriched with about 0.5 g/L of glucose. This was done to favor the establishment
5 of anoxic metabolic conditions in column B. Column experiments were performed at the
6 laboratory under room temperature conditions (22.7 ± 2.1 °C, average value \pm standard
7 deviation, 4 measures per week). Main composition and physical-chemical properties of the
8 inlet solutions are summarized in Table 1.



9

10 Fig. 1. Design of columns A and B (the dashed area shows the samples used for chemical
11 extractions).

12

13 2.3 Water quality monitoring

14 Inlet and outlet values of pH, redox potential (Eh), and dissolved oxygen (DO) were measured
15 twice per week by water probes. Water samples (about 40 mL) were collected from the inlet

1 and from the outlet of each column twice per week. Then, total phosphorus (TP), phosphate
2 ($\text{PO}_4\text{-P}$), total N (TN), chemical oxygen demand (COD), Al, Ca, and Fe concentrations of the
3 water samples were measured. TP concentrations were determined after persulfate digestion
4 (EN ISO6878, 2004), whereas $\text{PO}_4\text{-P}$, Al, Ca, and Fe concentrations were determined after
5 filtration ($0.45\ \mu\text{m}$ filters) of the water samples. Differences between TP removal efficiencies
6 of columns A and B were tested by the non-parametric Mann-Whitney U test, and were
7 considered significant at $p\text{-value} < 0.05$. Analytical and statistical methods are described in the
8 supplementary information (SI).

9 **2.4** *Chemical extractions*

10 A series of chemical extractions was performed to investigate the P content and chemical
11 changes of CBR before and after column experiments, and hence to elucidate the main P
12 removal mechanisms occurring in the columns. Samples of CBR were taken at the inlet-zone
13 of the columns A and B after 140 days of operation (Fig. 1). Since this zone was exposed to
14 inlet P-rich wastewater, these samples were likely to have had a high amount of P bound to
15 their surfaces. Before the chemical extractions, the samples of CBR were dried overnight at 45
16 °C to reduce water content and to avoid mineralogical changes deriving from high-temperature
17 drying [24].

18 *Aqua regia* extractions were performed according to standard methods (EN 13346, 2000; EN
19 13657, 2003) to determine the total P content of CBR before and after column experiments.

20 A series of chemical extractions was performed to quantify the amount of reactive amorphous
21 and crystalline Fe (hydro)xides and Al (hydro)xides on CBR samples before and after their use
22 in the columns. Indeed, speciation of reactive Fe and Al compounds in CBR may give useful
23 information to better understand and describe the P binding mechanisms [26]. Amorphous Fe,

1 crystalline Fe, and Al (hydro)xides extractions were performed according to standard method
2 ISO 12782-1 (2009), ISO 12782-2 (2009), and ISO 12782-3 (2009), respectively.

3 A sequential extraction protocol, adapted from Tiessen and Moir [27], was followed to quantify
4 the fractions of P bound to different mineral compounds in CBR before and after column
5 experiments. Four fractions of P were sequentially extracted from 1 g of CBR (dried mass
6 equivalent) following the procedure described in Barca *et al.* [28]:

7 i. Bicarbonate extractable inorganic P: this fraction is defined as weakly bound P, as P
8 extraction is mainly due to washing and ion exchange;

9 ii. Hydroxide extractable inorganic P: this fraction is primarily related to dissolution of Al
10 and Fe bound P compounds that are soluble at high pH;

11 iii. Diluted acid extractable inorganic P: this fraction is defined as Ca bound P, as P extraction
12 is mainly due to dissolution of Ca-P complexes at low pH;

13 iv. Hot concentrated acid extractable organic and inorganic P: this fraction represents P in
14 stable residual compounds that need much more energy to be dissolved.

15 The detailed protocols of the chemical extractions are presented and discussed in SI. All
16 chemical extractions were performed in duplicate or triplicate.

17 **3 Results and discussion**

18 **3.1 P removal performances**

19 The average values and standard deviations of inlet and outlet TP, PO₄-P, DO, pH, Eh, TN,
20 COD, Fe, Al, and Ca of columns A and B over day 1-54 (synthetic solution feeding) and day
21 55-140 of operation (real effluent feeding) are summarized in Table 1. A slight COD release
22 from column A was observed only during the first 3 weeks of operation, with outlet
23 concentrations up to 52 mg COD/L. This was primarily attributed to the use of organic

1 flocculants (polyacrylamide) during the dewatering process of bauxite residue [19]. For both
2 the columns, the average inlet TP concentration was 10.3 ± 0.5 mg P/L during the first period
3 of operation (synthetic solution feeding) and $5.5 \pm 1.5-1.7$ mg P/L during the second period of
4 operation (real effluent feeding). Results in Table 1 also indicate that $\text{PO}_4\text{-P}$ represent more
5 than 98% of inlet TP for synthetic solutions (day 1-54), and more than 89% of inlet TP for real
6 effluents (day 55-140). The difference between TP and $\text{PO}_4\text{-P}$ content in real effluents was
7 primarily attributed to stable organic P and P content in microorganisms [29]. Over the full
8 period of 140 days of operation, inlet and outlet DO concentrations of column A were 6.4 ± 1.0
9 mg $\text{O}_2\text{/L}$ and 2.3 ± 1.4 mg $\text{O}_2\text{/L}$, respectively, whereas inlet and outlet DO concentrations of
10 column B were 2.0 ± 3.2 mg $\text{O}_2\text{/L}$ and 0.3 ± 0.4 mg $\text{O}_2\text{/L}$, respectively, with outlet DO
11 stabilizing below a value of 0.3 mg $\text{O}_2\text{/L}$ after day 28 of operation (Fig. S1.B). These results
12 indicate that column A was operated under aerobic conditions during the full period of operation
13 (day 1-140), whereas column B was operated under anoxic conditions, this especially during
14 the second period of operation (day 55-140).

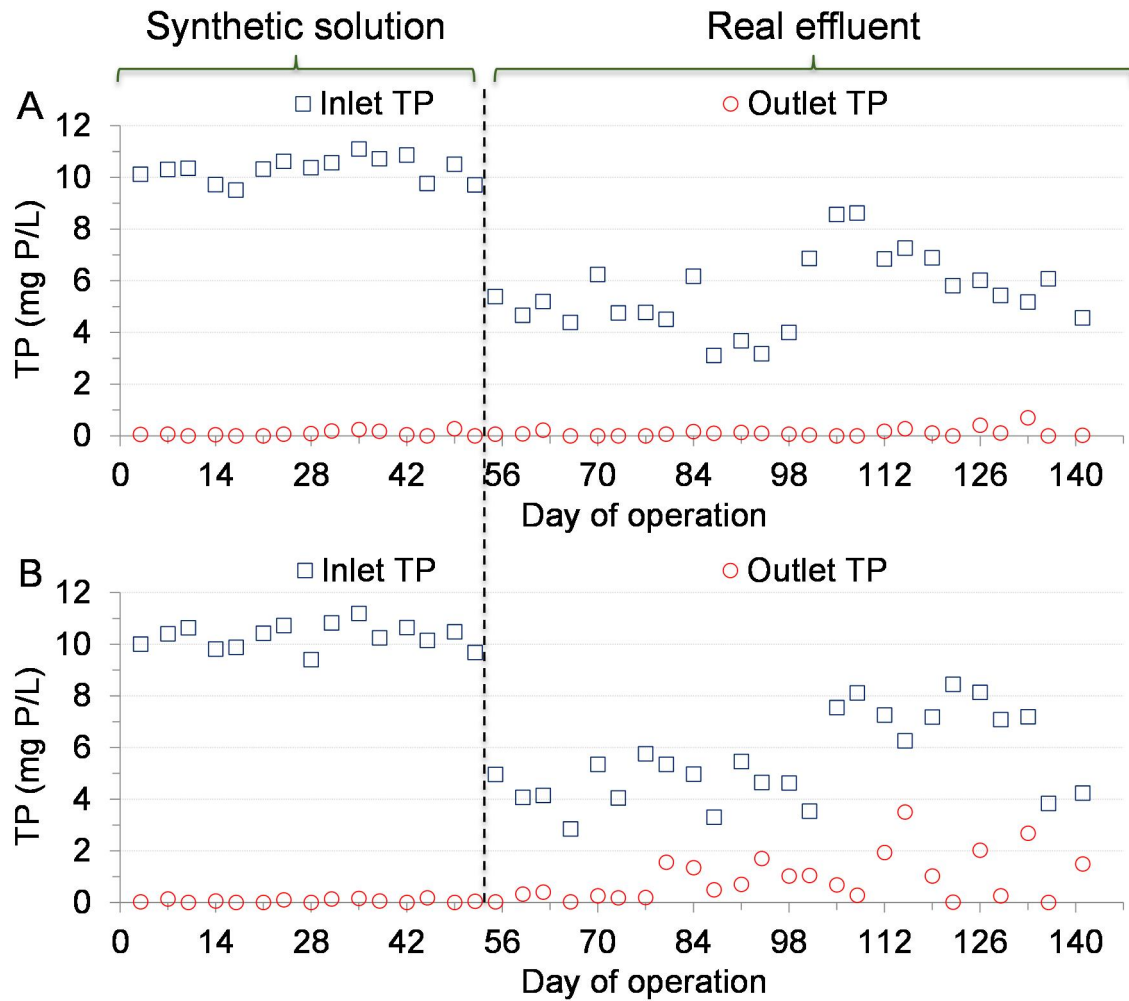
15

1 Table 1. Main water quality parameters at the inlet and at the outlet of columns A and B during
 2 day 1-54 (synthetic solution) and day 55-140 (real effluent feeding): average values \pm standard
 3 deviations (number of measurements).

Parameter	Column A		Column B	
	Day 1-54	Day 55-140	Day 1-54	Day 55-140
Inlet TP (mg P/L)	10.3 \pm 0.5 (15)	5.5 \pm 1.5 (25)	10.3 \pm 0.5 (15)	5.5 \pm 1.7 (25)
Outlet TP (mg P/L)	0.1 \pm 0.1 (15)	0.1 \pm 0.2 (25)	0.1 \pm 0.1 (15)	0.9 \pm 0.9 (25)
Inlet PO ₄ -P (mg P/L)	10.2 \pm 0.6 (15)	5.4 \pm 1.5 (25)	10.1 \pm 0.6 (15)	4.9 \pm 1.6 (25)
Outlet PO ₄ -P (mg P/L)	0.1 \pm 0.1 (15)	0.1 \pm 0.2 (25)	0.1 \pm 0.1 (15)	0.6 \pm 0.7 (25)
Inlet DO (mg O ₂ /L)	6.7 \pm 1.4 (13)	6.2 \pm 0.8 (25)	4.7 \pm 3.7 (13)	0.7 \pm 1.7 (25)
Outlet DO (mg O ₂ /L)	1.9 \pm 1.9 (13)	2.6 \pm 1.0 (25)	0.6 \pm 0.7 (13)	0.2 \pm 0.1 (25)
Inlet pH (-)	7.7 \pm 0.2 (15)	7.6 \pm 0.3 (25)	7.4 \pm 0.3 (15)	6.4 \pm 0.5 (25)
Outlet pH (-)	8.8 \pm 0.3 (15)	8.0 \pm 0.4 (25)	8.3 \pm 0.4 (15)	7.2 \pm 0.3 (25)
Inlet Eh (mV)	193 \pm 11 (15)	176 \pm 20 (25)	207 \pm 12 (15)	242 \pm 34 (25)
Outlet Eh (mV)	135 \pm 16 (15)	156 \pm 18 (25)	158 \pm 19 (15)	197 \pm 20 (25)
Inlet TN (mg N/L)	37.0 \pm 4.5 (8)	40.8 \pm 16.4 (13)	35.1 \pm 5.3 (8)	43.3 \pm 19.6 (13)
Outlet TN (mg N/L)	15.0 \pm 22.5 (8)	15.7 \pm 9.9 (13)	7.4 \pm 14.8 (8)	5.7 \pm 3.1 (13)
Inlet COD (mg O ₂ /L)	< 10 (3)	< 10 (3)	490 \pm 277 (8)	350 \pm 56 (13)
Outlet COD (mg O ₂ /L)	42 \pm 23 (5)	< 10 (4)	376 \pm 370 (8)	120 \pm 24 (13)
Inlet Fe (mg Fe/L)	< 0.01 (3)	0.02 \pm 0.03 (10)	0.08 \pm 0.09 (3)	0.11 \pm 0.04 (10)
Outlet Fe (mg Fe/L)	0.28 \pm 0.69 (7)	0.19 \pm 0.17 (10)	0.08 \pm 0.11 (7)	1.26 \pm 0.61 (10)
Inlet Al (mg Al/L)	< 0.01 (3)	0.72 \pm 1.80 (10)	0.08 \pm 0.13 (3)	0.07 \pm 0.22 (10)
Outlet Al (mg Al/L)	32.6 \pm 3.9 (7)	5.8 \pm 9.2 (10)	9.99 \pm 8.38 (7)	0.52 \pm 0.34 (10)
Inlet Ca (mg Ca/L)	92 \pm 5 (7)	265 \pm 63 (7)	120 \pm 20 (7)	268 \pm 8 (7)
Outlet Ca (mg Ca/L)	701 \pm 662 (7)	82 \pm 56 (7)	707 \pm 778 (7)	264 \pm 18 (7)

1 As shown in Fig. 2A, outlet TP concentrations of column A were always lower than 0.7 mg P/L
2 with an average value of 0.1 mg P/L. This indicates very high P removal efficiencies of column
3 A during the full period of operation (day 1-140). Over the first period of operation (day 1-55),
4 column B showed outlet TP concentrations always lower than 0.2 mg P/L, thus showing very
5 high P removal efficiencies (> 98%). However, a decrease in P removal performance of column
6 B was observed during the second period of operation (day 55-140), when an average outlet TP
7 concentration of 0.9 mg P/L and some massive releases of P (outlet TP > 2 mg P/L) were
8 observed (Fig. 2B). The results from non-parametric Mann-Whitney U tests (SI) indicate that
9 the differences between TP removal efficiencies of columns A and B were not significant during
10 day 1-54 of operation (p-value = 0.528), whereas they were significant during day 55-140 of
11 operation (p-value < 0.0001).

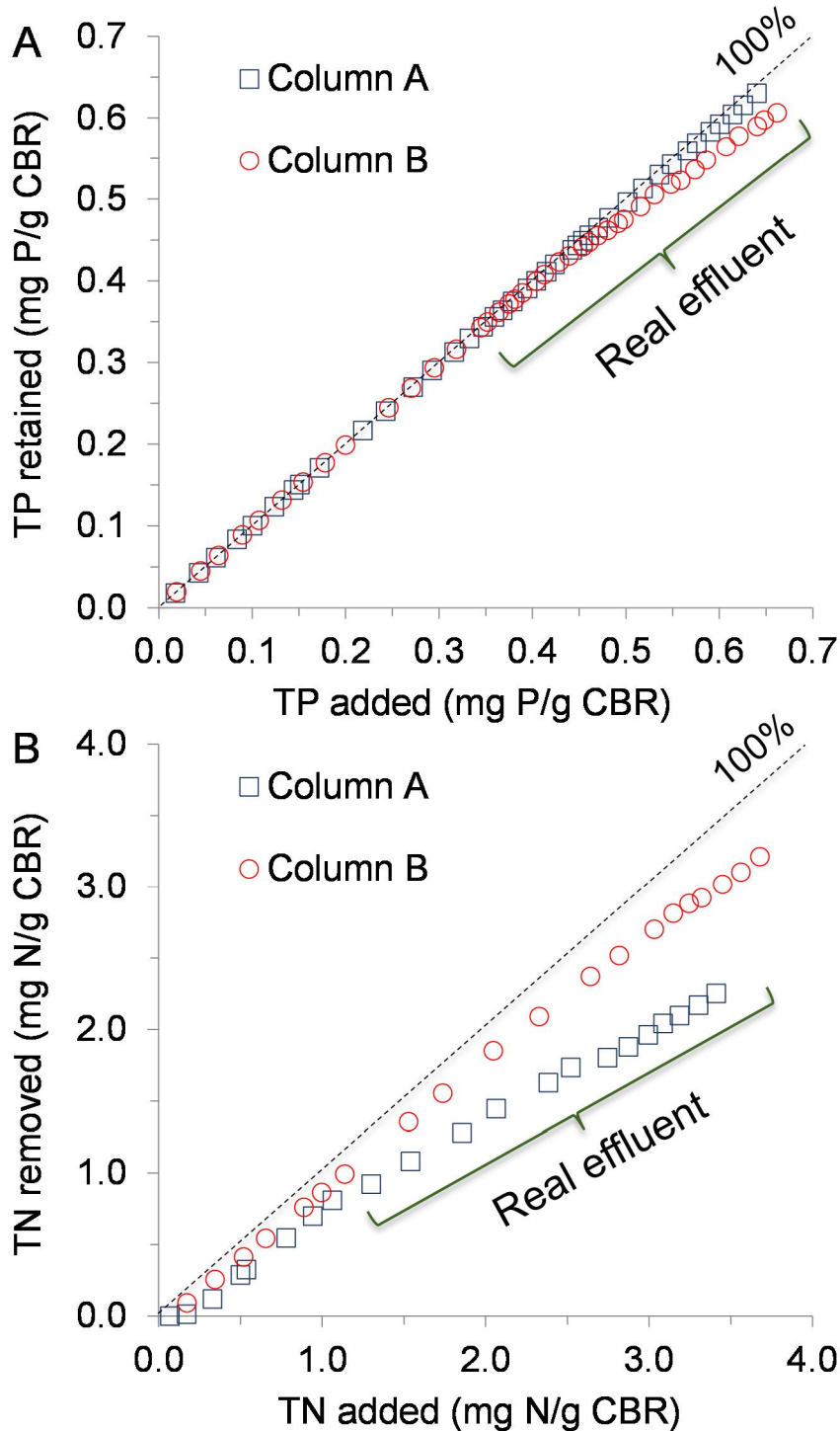
12



1
2 Fig. 2. Evolution of inlet and outlet TP concentrations: (A) column A; (B) column B.

3
4 Fig. 3A shows the evolution of TP retained as a function of TP added at the inlet of each column
5 (mg P/g CBR). Over the full period of 140 days of operation, column A showed a TP removal
6 performance of 98.5% and it reached a TP retention capacity of 0.63 mg P/g CBR, whereas
7 column B showed a TP removal performance of 91.6% and it reached a TP retention capacity
8 of 0.61 mg P/g CBR. As shown in Fig. 3A, P removal performance of column B has started to
9 decline during the second period of operation (day 55-140), when the column B was fed with a
10 real CW effluent enriched with glucose to promote anoxic biotic conditions inside the column.
11 Overall, these results suggest that the development of anoxic biotic conditions during the

1 operation of column B may account for its lower P removal performance, as described in the
2 following sections.



3
4 Fig. 3. Cumulated treatment performances of columns A and B over the full period of operation:
5 (A) TP retained as a function of TP added; (B) TN removed as a function of TN added.

1 COD and TN removal were studied to investigate the main metabolic processes occurring in
2 the columns. Fig. 3B shows the evolution of TN removed as a function of TN added to the inlet
3 of the columns A and B (mg N/g CBR). Over the full period of 140 days of operation, columns
4 A and B removed 66.1% and 87.3% of TN added to the inlet of each column, respectively. TN
5 removal in column A was, most probably, primarily related to adsorption of nitrate (NO_3^-) on
6 functional groups (*e.g.* $-\text{OH}$) at the surface of CBR [17], as already described by Cengeloglu *et*
7 *al.* [30]. As shown in Fig. 3B, TN removal performance of column A started to decline after 55
8 days of operation, thus suggesting saturation of adsorption sites. Instead, column B showed a
9 higher TN removal performance over the full period of operation. Most probably, glucose
10 addition and low DO concentrations promoted heterotrophic denitrification in column B, thus
11 improving TN removal performance. Inlet and outlet DO, COD, and TN concentrations of
12 column B (Table 1) appears to confirm that TN removal was related to COD removal according
13 to the metabolic pathways of heterotrophic denitrification. Indeed, several studies in the
14 literature indicate that denitrification in CWs occurs when DO is below 0.5 mg O_2/L and the
15 mass ratio of organic carbon to NO_3^- is higher than 2.86 g COD/g N [23,31]. Furthermore, the
16 results of this study are in good agreement with the findings of previous pilot experiments [32],
17 which have shown that the addition of methanol as a carbon substrate for denitrification
18 improves the TN removal performance of Bauxsol pellets (seawater-neutralized bauxite
19 residues) by a factor of 2. Over the full period of 140 days of operation, inlet and outlet Eh
20 values for column B were 229 ± 32 mV and 182 ± 27 mV (Table 1), respectively. These results
21 appear to confirm reduction of electron acceptors (*e.g.* NO_3^-) during water filtration through the
22 column B. Moreover, experimental Eh values varied in the range of values that promote
23 denitrification in CWs [29,33].

24 Table 2 summarizes the main results of previous column studies that have investigated P
25 removal performances of various types of untreated and treated bauxite residue. P removal

1 performances varied from 56% to 98%, thus confirming that bauxite residue is an efficient filter
2 material to remove P from wastewater. However, it is difficult to compare the results of the
3 different studies because of the large discrepancy on experimental parameters, such as type of
4 bauxite residue, type of solution, inlet P concentration, and particle size. Comparative
5 experiments of Herron *et al.* [34] have indicated that P removal performance increases from
6 28% to 98% with decreasing particle size from < 12 to < 2 mm, most probably because the
7 lower particle size gives a higher specific surface available for P sorption. However, the lower
8 particle size can also result in lower pore size between the grains, thus reducing the hydraulic
9 conductivity of the filters [35]. In addition, various biological and physical-chemical
10 phenomena, including biofilm growth, retention of suspended solids, particle segregation,
11 precipitation and accumulation of precipitates, may further decrease the void volume and the
12 pore size [36], thus affecting the long-term hydraulic and treatment performances of the filters
13 and increasing the risk of clogging when treating real effluents. Therefore, Herron *et al.* [34]
14 recommended the < 6 mm as optimum particle-size in field scale applications. It should be also
15 noticed that many of the experiments were conducted for too short a period to evaluate long-
16 term performances of the filters [21,34]. Despland *et al.* [32] observed that P removal
17 performances of columns packed with Bauxsol pellets decreased from 95% to 80% and to 60%
18 after 5 and 6 months of operation, respectively, thus suggesting saturation of P retention
19 capacity. The results of our study indicate very high P removal performances over the full
20 period of 140 days of operation (especially for column A, 98.5%), and no clogging phenomena
21 were observed.

Table 2. Main results from column experiments that have tested P removal performances of treated and untreated bauxite residue: BP = Bauxsol Pellet; RMFC = Red Mud Filter Cake; UBR = Untreated Bauxite Residue; CBR = Carbonated Bauxite Residue.

Study	Experimental parameters				Experimental results				
	Volume (L)	Material	Size (mm)	Feeding solution	Inlet P (mg P/L)	Inlet flow (L/h)	Duration of experiments	P removal performance	P retention capacity (g P/kg material)
Despland <i>et al.</i> [32]	10	SBP	5 - 10	Secondary WWTP effluent	3.0 - 9.2	0.9	180 days	> 60% ^a	~ 2
Herron <i>et al.</i> [34]	1.15	RMFC	< 2	Synthetic P solution	6	14.5 ^b	30 min	98%	25 ^c
	1.15	RMFC	< 6	Synthetic P solution	6	29 ^b	30 min	56%	N.A.
	1.15	RMFC	< 12	Synthetic P solution	6	44.6 ^b	30 min	28%	N.A.
Cusack <i>et al.</i> [21]	0.03	UBR	< 0.5	Forest run-off	1.1	0.030	22.8 min ^d	95%	0.045 ^e
	0.03	UBR	< 0.5	Dairy soiled water	10.6	0.030	5.8 min ^d	95%	0.27 ^e
This study	0.35	CBR	< 2	Synthetic and real CW effluent	3.1 - 11.1	0.012	140 days	98.5%	0.63
	0.35	CBR	< 2	Synthetic and real CW effluent + glucose	2.8 - 11.2	0.012	140 days	91.6%	0.61

^aP removal performances decreased below 95% after 30 days, and below 60% after 180 days of continuous operation;

^bBased on article data;

^cMaximum retention capacity from batch isotherm experiments (Langmuir equation);

^dFiltration time to observe a breakthrough concentration of 5% of the inlet P concentration;

^eModelled maximum retention capacity as a function of filtration time.

1 3.2 Alkaline and metal leaching from CBR

2 Alkaline releases from both the columns were observed during the full period of
3 operation, with average outlet pH values of 8.3 ± 0.5 and 7.7 ± 0.6 for columns A and B,
4 respectively. These pH increases were secondarily attributed to release of residual diluted
5 Na_2CO_3 and mainly to CaCO_3 dissolution from CBR, according to equation (2) [37], as
6 already described in a recent study that has investigated the effect of gypsum treatment
7 on the leaching behavior of CBR [15].



9 The highest outlet pH values (from 8.5 to 9.1) were observed during the first 2 months of
10 operation (Fig. S2), then they stabilized around a value of 7.7 ± 0.1 and 7.2 ± 0.2 for
11 columns A and B, respectively, after day 100 of operation. Over the full period of
12 operation, column B showed lower outlet pH than column A. This was most probably
13 related to the production of organic acids during the metabolic conversion of glucose in
14 column B, which buffered the increase in pH due to CaCO_3 dissolution.

15 The evolution of Ca, Al, and Fe release rates ($\mu\text{g}/(\text{g CBR} \cdot \text{day})$) from columns A and B
16 was calculated by outlet to inlet mass balances using equation (3), where C_{outlet} indicates
17 the outlet metal concentration ($\mu\text{g}/\text{L}$), C_{inlet} the inlet metal concentration ($\mu\text{g}/\text{L}$), M the
18 dried mass of CBR in the column (g), and F the feeding flow (L/day).

$$19 \text{Releaserate} = \frac{(C_{\text{outlet}} - C_{\text{inlet}})}{M} * F \quad (3)$$

20 As shown in Fig. 4, positive values indicate metal release from CBR, whereas negative
21 values indicate metal retention on CBR. Massive releases of Ca ($> 1200 \text{ mg Ca}/\text{L}$) were
22 observed from both the columns during the first 3 weeks of operation (Fig. S3), and they
23 were most probably related to dissolution of CaCO_3 and/or unreacted $\text{CaSO}_4 \cdot 2\text{H}_2\text{O}$ from
24 CBR (equation 1 and 2). Then, the data clearly indicate Ca retention in column A since

1 day 42 of operation, with outlet Ca concentrations always lower than inlet Ca
2 concentrations. During the second period of operation (real effluent feeding), the molar
3 ratio of Ca removed to P removed in column A varied from 10.8 to 56.0 mol Ca/mol P.
4 These values are 6.5 to 56 times higher than Ca to P molar ratios of the most common
5 Ca-phosphates in wastewater treatment systems (1-1.67 mol Ca/mol P) [38], thus
6 suggesting co-precipitation of Ca-phosphates and Ca-carbonates under slightly basic
7 conditions (inlet pH 7.6 ± 0.3 , outlet pH 8.0 ± 0.4), as already found in previous studies
8 [16,39]. Differently from column A, results from column B do not indicate Ca retention
9 during the second period of operation (real effluent feeding), this although the Ca content
10 of the real CW effluent was not a limiting factor for Ca-P precipitation, as indicated by
11 the Ca to P molar ratios always higher than 34 mol Ca/mol P. Most probably, the lower
12 pH values of column B (inlet pH 6.4 ± 0.5 , outlet pH 7.2 ± 0.3) had the effect of limiting
13 Ca-phosphate and Ca-carbonate precipitation compared to column A. Indeed, solubility
14 of Ca-phosphate and Ca-carbonate drastically increases with decreasing pH below 8 [40].
15 However, the findings of Cusack *et al.* [21] indicate that P removal by surface
16 precipitation of Ca-phosphates can happen at almost neutral pH and without requiring the
17 consumption of Ca ions from the inlet wastewater, as the result of the interaction between
18 $\text{PO}_4\text{-P}$ ions present in the wastewater with Ca-compounds already present in the
19 composition of bauxite residue.

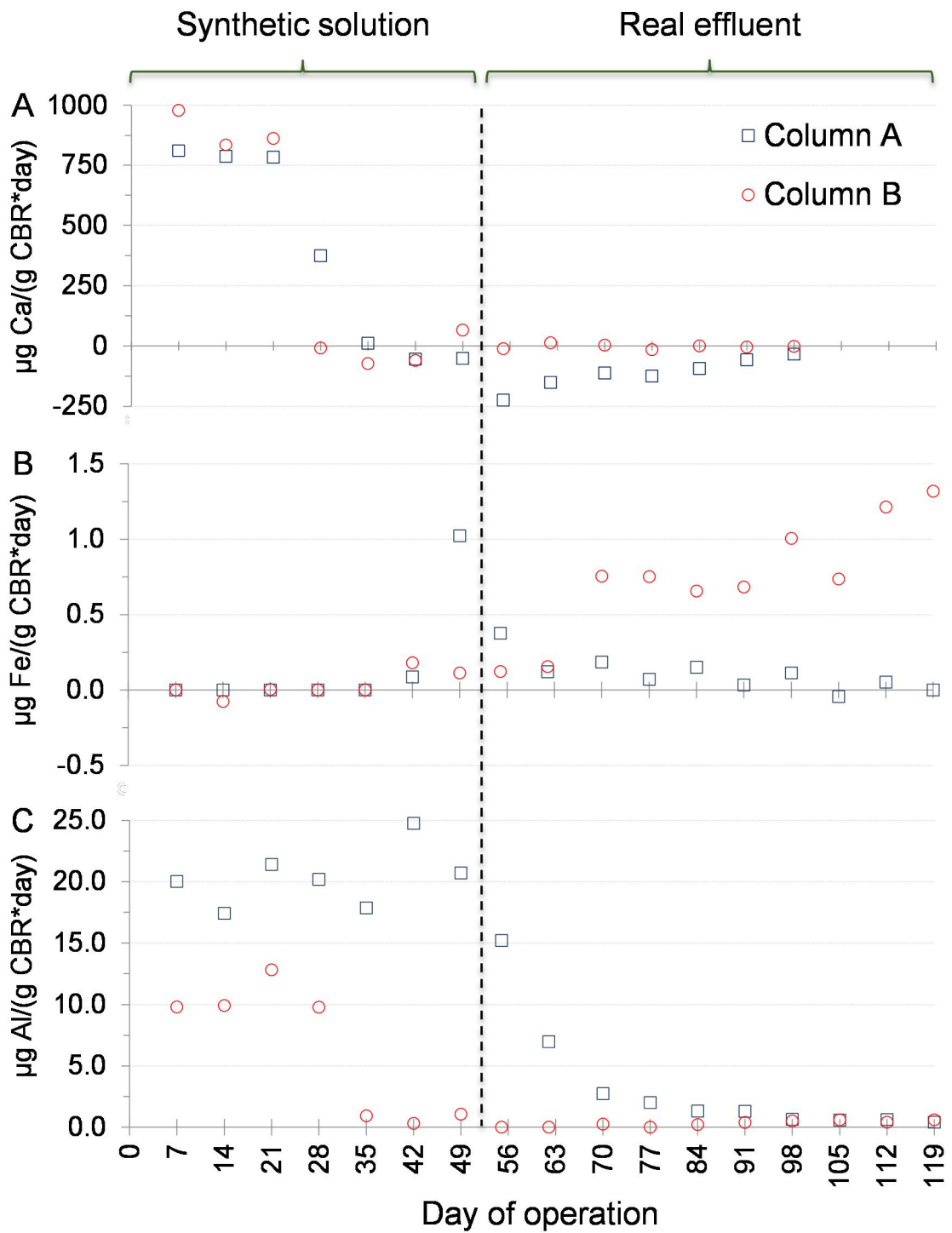
20 Massive releases of Al from CBR were observed during the first period of operation (day
21 1-55) (Fig. 4C), with outlet Al concentration exceeding 30 mg Al/L and 15 mg Al/L for
22 columns A and B, respectively (Fig. S4). These Al concentrations are several orders of
23 magnitude higher than the maximum theoretical solubility of Al-hydroxides in water for
24 pH ranging between 7-8 at 20 °C (0.3 mg Al/L, according to [41]). Therefore, they were

1 primarily attributed to washing out from the columns of colloidal fractions and/or very
2 fine Al-CBR particles passing the 0.45 μm filters. Then, outlet Al concentrations
3 stabilized below a value of 1 mg Al/L after day 98 and after day 49 of operation for
4 columns A and B, respectively. Lower outlet Al concentrations of column B were most
5 probably related to the more neutral values of outlet pH compared to column A (Table 1),
6 as it is well known from the literature that Al-hydroxides present minimum solubility at
7 pH ranging between 6-7 [41].

8 With the only exception of day 49, column A showed very few Fe releases during the full
9 period of operation (Fig. 4B), with outlet Fe concentrations lower than 0.3 mg Fe/L (Fig.
10 S5). The higher outlet Fe concentration on day 49 was most probably affected by a
11 cleaning step of the outlet pipe that likely had the effect of mobilizing and washing out
12 from the column some fine particles of CBR. Differently from column A, column B
13 showed higher Fe releases during the second period of operation (real effluent feeding),
14 with outlet Fe concentrations up to 2.1 mg Fe/L.

15 These results on metal release are in good agreement with the findings of Cusack *et al.*
16 [21], who observed Al and Fe releases from bauxite residue in rapid, small-scale column
17 tests with outlet Al and Fe concentrations up to 3.5 and 3 mg/L, respectively. Therefore,
18 they recommended a washing step before packing bauxite residue to prevent excessive
19 Al and Fe releases from the filters.

20



1

2 Fig. 4. Evolution of element release rates from columns A and B during the full period of
 3 operation: Ca release rate (A), Fe release rate (B), and Al release rate (C).

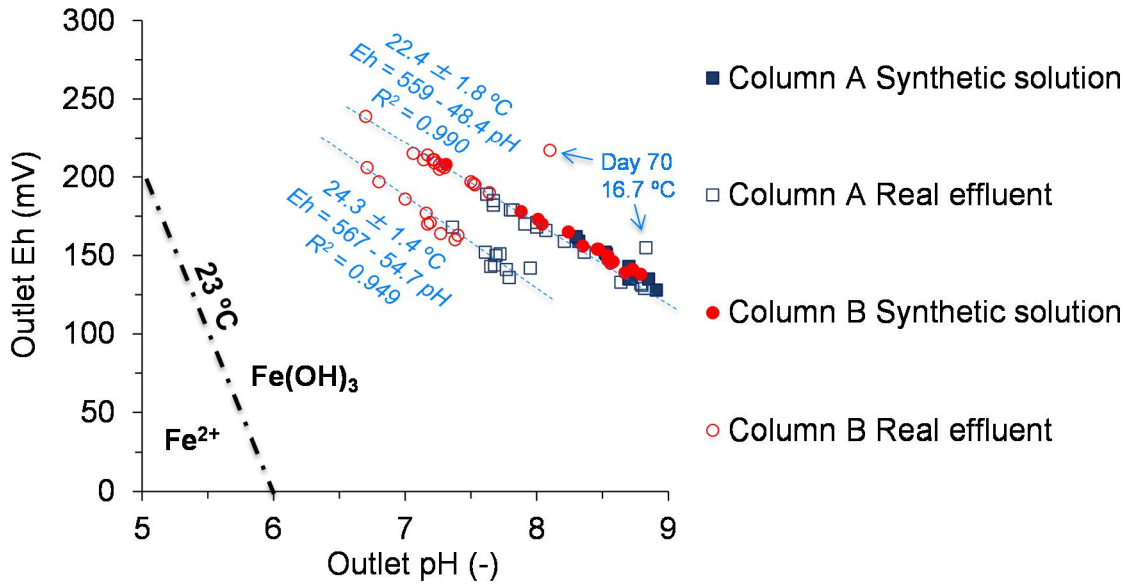
4

1 3.3 Iron mobilization in CBR

2 The results of our study seem to indicate Fe mobilization from CBR in column B under
3 anoxic biotic conditions, thus giving Fe releases up to 2.1 mg Fe/L. Both Eh and pH
4 values are commonly used as key parameters to evaluate redox conditions and to interpret
5 metal solubility data in soils [42,43]. The relationship between outlet Eh and pH for
6 columns A and B during the full period of operation is presented in Fig. 5 (Pourbaix
7 diagram, [44]). The results indicate a very good linear correlation between the
8 experimental data ($R^2 > 0.949$), with Eh increasing with decreasing the pH. These Eh-pH
9 relationships are in very good agreement with the findings of Husson *et al.* [42], who
10 concluded that both Eh and pH should be interactively used as relevant primary
11 parameters to characterize redox conditions in soils. As shown in Fig. 5, outlet Eh and pH
12 values varied between the ranges of values that promote solid-phase Fe hydroxides
13 ($\text{Fe}(\text{OH})_3$) at 23 °C, which was the average temperature during column experiments
14 (adapted from [45]). However, it should be noticed that theoretical $\text{Fe}^{3+}/\text{Fe}^{2+}$ equilibrium
15 conditions in Fig. 5 are established for $\text{Fe}(\text{OH})_3$ solution in pure water. The presence of
16 organic matter and/or microorganisms, and the related microbial activities, can play a key
17 role in Fe mobilization from solid matrices [26,46–48]. Under anoxic conditions,
18 microorganisms can use Fe^{3+} as a terminal electron acceptor to oxidize organic matter
19 during the anaerobic respiration process, thus reducing Fe^{3+} to more soluble Fe^{2+} .
20 Moreover, microorganisms can produce Fe^{3+} chelating molecules (*e.g.* siderophores) to
21 improve the bio-availability of soluble Fe^{3+} compounds from crystalline Fe^{3+} minerals
22 [46]. Overall, this microbially driven process of Fe^{3+} chelation and reduction can result
23 in the mobilization of soluble Fe^{3+} compounds and release of Fe^{2+} ions. The results in Fig.
24 5 also suggest a shift from more oxidizing to less oxidizing conditions with increasing

1 temperature from 16.7 to 24.3 °C, probably because the increase in temperature has a
 2 positive effect on microbial activity and a negative effect on oxygen saturation
 3 concentration.

4



5

6 Fig. 5. Simplified iron Pourbaix diagram at 23 °C (adapted from [45]). Outlet Eh and pH
 7 values of columns A and B over the full period of 140 days of operation.

8

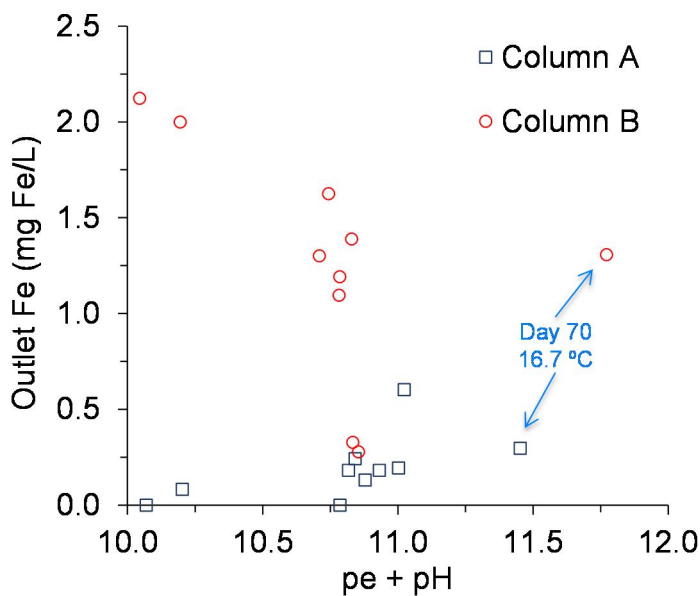
9 The chemical notion of $pe + pH$, which involves both the Eh and pH parameters, can be
 10 used as an indicator of the electronic activity of a solution in the presence of living
 11 organisms [42,43,48]. The electronic potential (pe) at 25 °C can be calculated from Eh
 12 (mV) by using equation (4).

13
$$pe = \frac{Eh}{59} \tag{4}$$

14 According to Husson *et al.* [42], at 25 °C pure water is redox indifferent at $pe + pH$ equal
 15 to 13.8. Then, $pe + pH$ values higher than 13.8 indicate oxidizing media, whereas $pe +$
 16 pH values lower than 13.8 indicate reducing media. The Fig. 6 shows the relationship

1 between Fe concentrations and pe + pH values of the effluents from columns A and B
 2 during the second period of operation (real effluent feeding), when Fe release was
 3 observed at the outlet of column B. For column B, the results indicate a clear trend of
 4 increase in outlet Fe concentration with decreasing pe + pH below a value of 11, whereas
 5 no correlations were observed between outlet Fe concentrations and pe + pH values in
 6 column A. These results appear to confirm Fe mobilization from CBR in the presence of
 7 living microorganisms under anoxic conditions (column B).

8



9

10 Fig. 6. Outlet Fe concentrations of columns A and B as a function of pe + pH during day
 11 55-140 of operation (real effluent feeding).

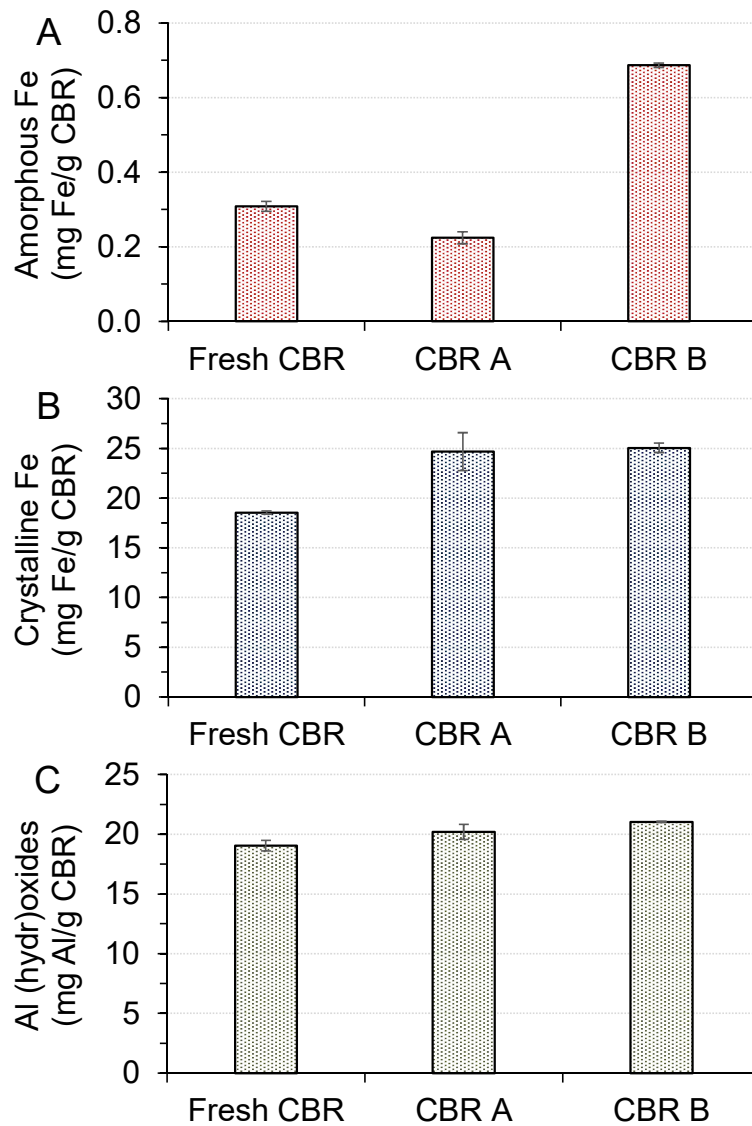
12

13 Fig. 7 summarizes the results of amorphous Fe, crystalline Fe, and Al (hydr)oxide
 14 extractions from CBR before (Fresh CBR) and after their use as filter substrate in the
 15 columns A and B (CBR A and CBR B, respectively). The results indicate a relative
 16 increase in crystalline Fe and Al (hydr)oxides for both the columns after 140 days of

1 operation (Fig. 7B and C). These relative increases in crystalline Fe and Al (hydr)oxide
2 contents were most probably related to the dissolution of more soluble Ca-compounds
3 from CBR (*e.g.* CaCO₃ and residual gypsum), as already suggested by the high Ca
4 releases observed during the first month of column operation (Fig. 4A).

5 As shown in Fig. 7A, the results indicate a slight decrease in amorphous Fe for column A
6 after 140 days of operation, which was most probably related to washing out from the
7 column of more mobile Fe compounds. Differently from column A, the content of
8 amorphous Fe in column B (CBR B) increased by a factor 2.2 compared to fresh CBR,
9 thus suggesting the conversion of crystalline Fe to amorphous Fe compounds under
10 anoxic biotic conditions. The conversion of crystalline Fe to amorphous Fe compounds
11 was already observed in soils in the presence of living microorganisms [26,47,48], and it
12 was primarily attributed to microbial reduction of crystalline Fe³⁺ (hydr)oxides probably
13 followed by the precipitation of amorphous Fe²⁺ complexes [47]. Li *et al.* [48] observed
14 that a decrease of pe + pH from 11.06 to 8.29 was accompanied by a 110% increase of
15 amorphous Fe content in rhizosphere soils. According to the authors, low pe + pH may
16 promote the activity of Fe reduction bacteria to produce Fe²⁺, which is re-oxidized to
17 amorphous Fe oxides. However, this hypothesis still needs to be verified by further
18 studies [48].

19



1

2 Fig. 7. Amorphous Fe (A), crystalline Fe (B), and Al (hydr)oxide extraction (C) from
 3 CBR before (Fresh CBR) and after 140 days of column operation (CBR A and CBR B).
 4 Average values from triplicate (amorphous Fe) and duplicate (crystalline Fe and Al
 5 (hydr)oxides) experiments, bars indicating the range min-max values.

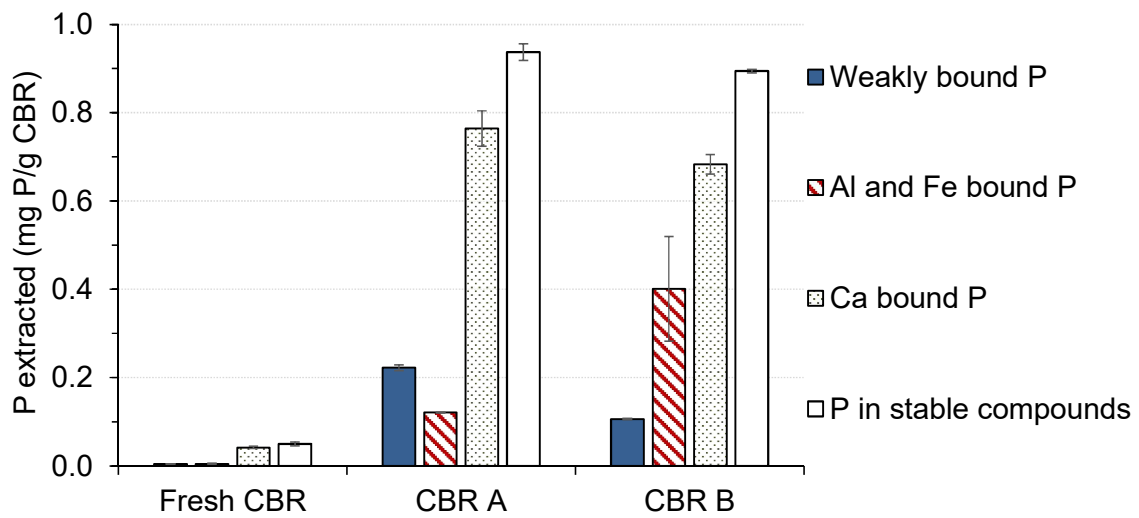
6

7 3.4 P removal mechanisms

8 The results of sequential P extractions from CBR samples before (Fresh CBR) and after
 9 140 days of column operation (CBR A and CBR B) are summarized in Fig. 8. The total

1 amounts of P extracted by sequential extractions was 0.10 ± 0.01 mg P/kg CBR, $2.04 \pm$
 2 0.04 mg P/kg CBR, and 2.08 ± 0.21 mg P/kg CBR for Fresh CBR, CBR A and CBR B,
 3 respectively (average values \pm standard deviations from duplicate experiments), thus
 4 confirming P retention on CBR during column experiments, and indicating a similar total
 5 amount of P extracted from CBR A and CBR B.

6



7

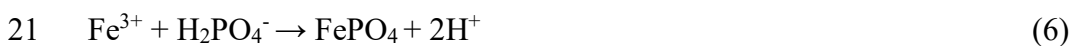
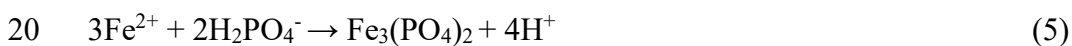
8 Fig. 8. Sequential extraction experiments: P fractions extracted from CBR before (Fresh
 9 CBR) and after 140 days of column operation (CBR A and CBR B). Average values from
 10 duplicates, bars indicating the range min-max values.

11

12 P in stable residual compounds represents the 45.8% and 42.9% of total P extracted from
 13 CBR A and CBR B, respectively, followed by Ca bound P that represents the 37.4% and
 14 32.8% of total P extracted from CBR A and CBR B, respectively (Fig. 8). In the literature
 15 [27,28,49], P in stable residual compounds is mainly attributed to the most
 16 thermodynamically stable Ca-P crystals (*e.g.* hydroxyapatite) and/or organic matter that
 17 is not alkali extractable (organic P), whereas Ca bound P is mainly attributed to

1 amorphous Ca phosphates that can be dissolved with diluted acids (e.g. 1 M HCl). These
2 results seem to confirm that Ca-P precipitation followed by the retention of Ca-P
3 complexes into the columns was the main mechanism leading to P removal from
4 wastewater, as already observed in previous column studies that have investigated P
5 removal performances of Ca rich filter substrates (steel slag) [39,50,51]. Their findings
6 indicated that Ca phosphates initially precipitate under amorphous forms, and later
7 recrystallize into the most thermodynamically stable form of hydroxyapatite.

8 As shown in Fig. 8, Al and Fe bound P extracted from CBR B (0.40 ± 0.17 mg P/g CBR)
9 was 3.3 times higher than Al and Fe bound P extracted from CBR A (0.12 ± 0.01 mg P/g
10 CBR). The higher amorphous Fe content in CBR B appears to be correlated with the
11 higher Al and Fe bound P in CBR B, when comparing Fe and P extraction data from CBR
12 A and CBR B. Moreover, the molar ratio of Fe to P between the differences of (i)
13 amorphous Fe in CBR B and A (Fig. 7), and (ii) Al and Fe bound P in CBR B and A (Fig.
14 8), is equal to 0.92 mol Fe/mol P. This value is close to the theoretical Fe/P ratios of the
15 most common Fe-P complexes in wastewater systems (1-1.5 mol Fe/mol P). These results
16 may indicate re-precipitation of mobilized Fe as amorphous Fe-P phases on CBR B at
17 almost neutral pH (equation 5 and 6), as already observed and described in previous
18 studies that have investigated the effects of microbial driven Fe mobilization in soils
19 [26,47].



22 The results of *aqua regia* extractions indicate total P contents of 2.66 ± 0.05 mg P/kg
23 CBR and 3.00 ± 0.10 mg P/kg CBR for CBR A and CBR B, respectively (average values
24 \pm standard deviations from duplicate experiments). These values are 30% and 44% higher

1 than the total amounts of P extracted by sequential extractions for CBR A and CBR B,
2 respectively. According to Tiessen and Moir [27], these differences may be related to
3 highly recalcitrant inorganic P, but also to bicarbonate and hydroxide extractable organic
4 P that were not taken into account in sequential extractions. Most probably, biological P
5 uptake in column B may explain the higher difference between total P extracted by *aqua*
6 *regia* and total amount of P extracted by sequential extraction for CBR B.

7 **3.5** *Closing remarks and perspectives*

8 Overall, the results of this study indicate that aeration conditions and microbial activity
9 affect the performance and P removal mechanisms of CBR filters as follows. Under
10 aerobic conditions, Ca-P precipitation (probably followed by crystallization of Ca-P
11 complexes) on the surface of CBR appears to be the main mechanism leading to P
12 removal from wastewater. Under anoxic biotic conditions, microbially driven
13 mobilization of Fe from minerals may (i) provide Fe ions for further Fe-P precipitation,
14 but also may (ii) lead to Fe releases from CBR filters.

15 Vertical flow CWs represent one of the most employed wastewater treatment systems for
16 small communities in France (less than 2000 people equivalent), with more than 2500
17 systems in operation in 2015 [25]. According to Paing *et al.* [25], French vertical flow
18 CWs present high removal performances for COD and total suspended solids (TSS),
19 whereas TP and TN removal performances are relatively low (mean values of 151 plants:
20 93%, 96%, 30% and 39% for COD, TSS, TP, and TN removal, respectively). Therefore,
21 the use of CBR filters appears to be particularly suitable as a tertiary treatment step to
22 remove P from the effluents of vertical flow CWs. The addition of external organic carbon
23 and/or partial recirculation of raw wastewater at the inlet of CBR filters can further
24 improve TN removal by coupling the processes of P retention and denitrification in a

1 single treatment step, but could also promote Fe mobilization and give a lower TP
2 removal performance.

3 However, further studies are needed before full-scale application of CBR filters in CWs.
4 In particular, long-term pilot experiments at the field-scale are required to evaluate the
5 effects of seasonal variations of wastewater temperature and composition, and
6 accumulation of solids and precipitates, on the hydraulic and treatment performances of
7 CBR filters under real operating conditions.

8 **4 Conclusions**

9 The results of this study confirm that CBR is an efficient filter material to remove P from
10 wastewater. Over 140 days of operation, column A showed a TP removal performance of
11 98.5% achieving a TP retention capacity of 0.63 mg P/g CBR, whereas column B showed
12 a TP removal performance of 91.6% achieving a TP retention capacity of 0.61 mg P/g
13 CBR, thus indicating higher P removal performance of CBR under aerobic rather than
14 anoxic biotic conditions. The main mechanisms of P removal were related to the
15 precipitation of Ca-P complexes, most probably followed by recrystallization under more
16 stable forms (*e.g.* hydroxyapatite) on the mineral surface of CBR. The results of this study
17 also indicate Fe mobilization from CBR under anoxic biotic conditions, thus (i) providing
18 Fe ions that are available for further Fe-P precipitation, but also (ii) leading to Fe releases
19 from CBR filters. Overall, the results of this study indicate that CBR filters can be
20 successfully applied to remove P from effluents with low organic load in both aerobic as
21 well as anoxic conditions, but aerobic conditions are recommended to prevent excessive
22 Fe release from CBR.

23 **Acknowledgements**

1 This work was cofunded by ALTEO and the Labex DRIIHM, French program
2 "Investissements d'Avenir" (ANR-11-LABX-0010) which is managed by the ANR.

3 **Supplementary information**

4 Fig. S1. Evolution of inlet and outlet DO concentrations: (A) column A; (B) column B.

5 Fig. S2. Evolution of inlet and outlet pH: (A) column A; (B) column B.

6 Fig. S3. Evolution of inlet and outlet Ca concentrations: (A) column A; (B) column B.

7 Fig. S4. Evolution of inlet and outlet Al concentrations: (A) column A; (B) column B.

8 Fig. S5. Evolution of inlet and outlet Fe concentrations: (A) column A; (B) column B.

9 Table S1. Statistical analysis of TP removal efficiencies of columns A and B.

10 Table S2. Main results of the non-parametric Mann-Whitney U tests comparing TP
11 removal efficiencies of columns A and B.

12 **References**

- 13 [1] J.T. Bunce, E. Ndam, I.D. Ofiteru, A. Moore, D.W. Graham, A Review of
14 Phosphorus Removal Technologies and Their Applicability to Small-Scale
15 Domestic Wastewater Treatment Systems, *Front. Environ. Sci.* 6 (2018).
16 <https://doi.org/10.3389/fenvs.2018.00008>.
- 17 [2] X. Shi, J. Fan, J. Zhang, Y. Shen, Enhanced phosphorus removal in intermittently
18 aerated constructed wetlands filled with various construction wastes, *Environ Sci*
19 *Pollut Res.* 24 (2017) 22524–22534. <https://doi.org/10.1007/s11356-017-9870-z>.
- 20 [3] Y. Gao, W. Zhang, B. Gao, W. Jia, A. Miao, L. Xiao, L. Yang, Highly efficient
21 removal of nitrogen and phosphorus in an electrolysis-integrated horizontal
22 subsurface-flow constructed wetland amended with biochar, *Water Research.* 139
23 (2018) 301–310. <https://doi.org/10.1016/j.watres.2018.04.007>.
- 24 [4] J. Barak, G. Dotro, B. Jefferson, The role of concentrations gradients on phosphorus
25 and iron dynamics from chemically-dosed horizontal flow wetlands for tertiary
26 sewage treatment, *Water Sci Technol.* 79 (2019) 2126–2134.
27 <https://doi.org/10.2166/wst.2019.215>.
- 28 [5] C. Maucieri, M. Salvato, M. Borin, Vegetation contribution on phosphorus removal
29 in constructed wetlands, *Ecological Engineering.* 152 (2020) 105853.
30 <https://doi.org/10.1016/j.ecoleng.2020.105853>.
- 31 [6] Y. Wang, Z. Cai, S. Sheng, F. Pan, F. Chen, J. Fu, Comprehensive evaluation of
32 substrate materials for contaminants removal in constructed wetlands, *Science of*
33 *The Total Environment.* 701 (2020) 134736.
34 <https://doi.org/10.1016/j.scitotenv.2019.134736>.

- 1 [7] S. Adera, A. Drizo, E. Twohig, K. Jagannathan, G. Benoit, Improving Performance
2 of Treatment Wetlands: Evaluation of Supplemental Aeration, Varying Flow
3 Direction, and Phosphorus Removing Filters, *Water Air Soil Pollut.* 229 (2018) 100.
4 <https://doi.org/10.1007/s11270-018-3723-3>.
- 5 [8] C. Barca, S. Troesch, D. Meyer, P. Drissen, Y. Andrès, F. Chazarenc, Steel Slag
6 Filters to Upgrade Phosphorus Removal in Constructed Wetlands: Two Years of
7 Field Experiments, *Environ. Sci. Technol.* 47 (2013) 549–556.
8 <https://doi.org/10.1021/es303778t>.
- 9 [9] D. Claveau-Mallet, É. Boutet, Y. Comeau, Steel slag filter design criteria for
10 phosphorus removal from wastewater in decentralized applications, *Water
11 Research.* 143 (2018) 28–37. <https://doi.org/10.1016/j.watres.2018.06.032>.
- 12 [10] N. Harouiya, S. Martin Rue, S. Prost-Boucle, A. Liénar, D. Esser, P. Molle,
13 Phosphorus removal by apatite in horizontal flow constructed wetlands for small
14 communities: pilot and full-scale evidence, *Water Science and Technology.* 63
15 (2011) 1629–1637. <https://doi.org/10.2166/wst.2011.250>.
- 16 [11] H. Bacelo, A.M.A. Pintor, S.C.R. Santos, R.A.R. Boaventura, C.M.S. Botelho,
17 Performance and prospects of different adsorbents for phosphorus uptake and
18 recovery from water, *Chemical Engineering Journal.* 381 (2020) 122566.
19 <https://doi.org/10.1016/j.cej.2019.122566>.
- 20 [12] G. Ezzati, M.G. Healy, L. Christianson, K. Daly, O. Fenton, G. Feyereisen, S.
21 Thornton, O. Callery, Use of rapid small-scale column tests for simultaneous
22 prediction of phosphorus and nitrogen retention in large-scale filters, *Journal of
23 Water Process Engineering.* 37 (2020) 101473.
24 <https://doi.org/10.1016/j.jwpe.2020.101473>.
- 25 [13] C. Vohla, M. Kõiv, H.J. Bavor, F. Chazarenc, Ü. Mander, Filter materials for
26 phosphorus removal from wastewater in treatment wetlands—A review, *Ecological
27 Engineering.* 37 (2011) 70–89. <https://doi.org/10.1016/j.ecoleng.2009.08.003>.
- 28 [14] Y. Wang, Y. Yu, H. Li, C. Shen, Comparison study of phosphorus adsorption on
29 different waste solids: Fly ash, red mud and ferric–alum water treatment residues,
30 *Journal of Environmental Sciences.* 50 (2016) 79–86.
31 <https://doi.org/10.1016/j.jes.2016.04.025>.
- 32 [15] P.B. Cusack, M.G. Healy, P.C. Ryan, I.T. Burke, L.M.T. O’ Donoghue, É. Ujaczki,
33 R. Courtney, Enhancement of bauxite residue as a low-cost adsorbent for
34 phosphorus in aqueous solution, using seawater and gypsum treatments, *Journal of
35 Cleaner Production.* 179 (2018) 217–224.
36 <https://doi.org/10.1016/j.jclepro.2018.01.092>.
- 37 [16] R.A. Pepper, S.J. Couperthwaite, G.J. Millar, Re-use of waste red mud: Production
38 of a functional iron oxide adsorbent for removal of phosphorous, *Journal of Water
39 Process Engineering.* 25 (2018) 138–148.
40 <https://doi.org/10.1016/j.jwpe.2018.07.006>.
- 41 [17] Y. Zhao, Q. Yue, Q. Li, X. Xu, Z. Yang, X. Wang, B. Gao, H. Yu, Characterization
42 of red mud granular adsorbent (RMGA) and its performance on phosphate removal
43 from aqueous solution, *Chemical Engineering Journal.* 193–194 (2012) 161–168.
44 <https://doi.org/10.1016/j.cej.2012.04.040>.
- 45 [18] Y. Li, C. Liu, Z. Luan, X. Peng, C. Zhu, Z. Chen, Z. Zhang, J. Fan, Z. Jia, Phosphate
46 removal from aqueous solutions using raw and activated red mud and fly ash,
47 *Journal of Hazardous Materials.* 137 (2006) 374–383.
48 <https://doi.org/10.1016/j.jhazmat.2006.02.011>.

- 1 [19] K. Evans, The History, Challenges, and New Developments in the Management and
2 Use of Bauxite Residue, *Journal of Sustainable Metallurgy*. 2 (2016) 316–331.
3 <https://doi.org/10.1007/s40831-016-0060-x>.
- 4 [20] É. Ujaczki, V. Feigl, M. Molnár, P. Cusack, T. Curtin, R. Courtney, L. O’Donoghue,
5 P. Davris, C. Hugi, M.W. Evangelou, E. Balomenos, M. Lenz, Re-using bauxite
6 residues: benefits beyond (critical raw) material recovery, *Journal of Chemical
7 Technology & Biotechnology*. 93 (2018) 2498–2510.
8 <https://doi.org/10.1002/jctb.5687>.
- 9 [21] P.B. Cusack, O. Callery, R. Courtney, É. Ujaczki, L.M.T. O’Donoghue, M.G.
10 Healy, The use of rapid, small-scale column tests to determine the efficiency of
11 bauxite residue as a low-cost adsorbent in the removal of dissolved reactive
12 phosphorus from agricultural waters, *Journal of Environmental Management*. 241
13 (2019) 273–283. <https://doi.org/10.1016/j.jenvman.2019.04.042>.
- 14 [22] S. Lu, H. Hu, Y. Sun, J. Yang, Effect of carbon source on the denitrification in
15 constructed wetlands, *Journal of Environmental Sciences*. 21 (2009) 1036–1043.
16 [https://doi.org/10.1016/S1001-0742\(08\)62379-7](https://doi.org/10.1016/S1001-0742(08)62379-7).
- 17 [23] H. Ilyas, I. Masih, The performance of the intensified constructed wetlands for
18 organic matter and nitrogen removal: A review, *Journal of Environmental
19 Management*. 198 (2017) 372–383. <https://doi.org/10.1016/j.jenvman.2017.04.098>.
- 20 [24] M. Liira, M. Kõiv, Ü. Mander, R. Mõtsep, C. Vohla, K. Kirsimäe, Active Filtration
21 of Phosphorus on Ca-Rich Hydrated Oil Shale Ash: Does Longer Retention Time
22 Improve the Process?, *Environ. Sci. Technol.* 43 (2009) 3809–3814.
23 <https://doi.org/10.1021/es803642m>.
- 24 [25] J. Paing, A. Guilbert, V. Gagnon, F. Chazarenc, Effect of climate, wastewater
25 composition, loading rates, system age and design on performances of French
26 vertical flow constructed wetlands: A survey based on 169 full scale systems,
27 *Ecological Engineering*. 80 (2015) 46–52.
28 <https://doi.org/10.1016/j.ecoleng.2014.10.029>.
- 29 [26] J.P.M. Vink, A. van Zomeren, J.J. Dijkstra, R.N.J. Comans, When soils become
30 sediments: Large-scale storage of soils in sandpits and lakes and the impact of
31 reduction kinetics on heavy metals and arsenic release to groundwater,
32 *Environmental Pollution*. 227 (2017) 146–156.
33 <https://doi.org/10.1016/j.envpol.2017.04.016>.
- 34 [27] H. Tiessen, J.O. Moir, Characterization of available P by sequential extraction, *Soil
35 Sampling and Methods of Analysis*. 7 (1993) 5–229.
- 36 [28] C. Barca, M. Martino, P. Hennebert, N. Roche, Kinetics and capacity of phosphorus
37 extraction from solid residues obtained from wet air oxidation of sewage sludge,
38 *Waste Management*. 89 (2019) 275–283.
39 <https://doi.org/10.1016/j.wasman.2019.04.024>.
- 40 [29] J. Vymazal, Removal of nutrients in various types of constructed wetlands, *Science
41 of The Total Environment*. 380 (2007) 48–65.
42 <https://doi.org/10.1016/j.scitotenv.2006.09.014>.
- 43 [30] Y. Cengeloglu, A. Tor, M. Ersoz, G. Arslan, Removal of nitrate from aqueous
44 solution by using red mud, *Separation and Purification Technology*. 51 (2006) 374–
45 378. <https://doi.org/10.1016/j.seppur.2006.02.020>.
- 46 [31] F. Ye, Y. Li, Enhancement of nitrogen removal in towery hybrid constructed
47 wetland to treat domestic wastewater for small rural communities, *Ecological
48 Engineering*. 35 (2009) 1043–1050. <https://doi.org/10.1016/j.ecoleng.2009.03.009>.

- 1 [32] L.M. Despland, M.W. Clark, T. Vancov, D. Erler, M. Aragno, Nutrient and Trace-
2 Metal Removal by Bauxsol Pellets in Wastewater Treatment, *Environmental*
3 *Science & Technology*. 45 (2011) 5746–5753. <https://doi.org/10.1021/es200934y>.
- 4 [33] D.D. Silveira, P. Belli Filho, L.S. Philippi, B. Kim, P. Molle, Influence of partial
5 saturation on total nitrogen removal in a single-stage French constructed wetland
6 treating raw domestic wastewater, *Ecological Engineering*. 77 (2015) 257–264.
7 <https://doi.org/10.1016/j.ecoleng.2015.01.040>.
- 8 [34] S.L. Herron, A.N. Sharpley, K.R. Brye, D.M. Miller, Optimizing Hydraulic and
9 Chemical Properties of Iron and Aluminum Byproducts for Use in On-Farm
10 Containment Structures for Phosphorus Removal, *Journal of Environmental*
11 *Protection*. 07 (2016) 1835–1849. <https://doi.org/10.4236/jep.2016.712146>.
- 12 [35] X.W. Ren, J.C. Santamarina, The hydraulic conductivity of sediments: A pore size
13 perspective, *Engineering Geology*. 233 (2018) 48–54.
14 <https://doi.org/10.1016/j.enggeo.2017.11.022>.
- 15 [36] C. Barca, N. Roche, S. Troesch, Y. Andrès, F. Chazarenc, Modelling hydrodynamics
16 of horizontal flow steel slag filters designed to upgrade phosphorus removal in small
17 wastewater treatment plants, *Journal of Environmental Management*. 206 (2018)
18 349–356. <https://doi.org/10.1016/j.jenvman.2017.10.040>.
- 19 [37] G. Kaufmann, D. Wolfgang, Calcite dissolution kinetics in the system CaCO_3 –
20 H_2O – CO_2 at high undersaturation, *Geochimica et Cosmochimica Acta*. 71 (2007)
21 1398–1410. <https://doi.org/10.1016/j.gca.2006.10.024>.
- 22 [38] E. Valsami-Jones, Mineralogical controls on phosphorus recovery from
23 wastewaters, *Mineralogical Magazine*. 65 (2001) 611–620.
24 <https://doi.org/10.1180/002646101317018433>.
- 25 [39] C. Barca, D. Meyer, M. Liira, P. Drissen, Y. Comeau, Y. Andrès, F. Chazarenc,
26 Steel slag filters to upgrade phosphorus removal in small wastewater treatment
27 plants: Removal mechanisms and performance, *Ecological Engineering*. 68 (2014)
28 214–222. <https://doi.org/10.1016/j.ecoleng.2014.03.065>.
- 29 [40] W. Stumm, J.J. Morgan, *Aquatic Chemistry: Chemical Equilibria and Rates in*
30 *Natural Waters*, John Wiley & Sons, 2012.
- 31 [41] D.J. Pernitsky, J.K. Edzwald, Selection of alum and polyaluminum coagulants:
32 principles and applications, *Journal of Water Supply: Research and Technology -*
33 *Aqua*. 55 (2006) 121–141. <https://doi.org/10.2166/aqua.2006.062>.
- 34 [42] O. Husson, B. Husson, A. Brunet, D. Babre, K. Alary, J.-P. Sarthou, H. Charpentier,
35 M. Durand, J. Benada, M. Henry, Practical improvements in soil redox potential
36 (Eh) measurement for characterisation of soil properties. Application for
37 comparison of conventional and conservation agriculture cropping systems,
38 *Analytica Chimica Acta*. 906 (2016) 98–109.
39 <https://doi.org/10.1016/j.aca.2015.11.052>.
- 40 [43] W.L. Lindsay, M. Sadiq, Use of pe + pH to predict and interpret metal solubility
41 relationships in soils, *Science of The Total Environment*. 28 (1983) 169–178.
42 [https://doi.org/10.1016/S0048-9697\(83\)80016-3](https://doi.org/10.1016/S0048-9697(83)80016-3).
- 43 [44] M. Pourbaix, *Atlas of electrochemical equilibria in aqueous solutions*, National
44 Association of Corrosion Engineers, 1974.
- 45 [45] H. Elnakar, I. Buchanan, Soluble chemical oxygen demand removal from bypass
46 wastewater using iron electrocoagulation, *Science of The Total Environment*. 706
47 (2020) 136076. <https://doi.org/10.1016/j.scitotenv.2019.136076>.

- 1 [46] C. Colombo, G. Palumbo, J.-Z. He, R. Pinton, S. Cesco, Review on iron availability
2 in soil: interaction of Fe minerals, plants, and microbes, *J Soils Sediments*. 14 (2014)
3 538–548. <https://doi.org/10.1007/s11368-013-0814-z>.
- 4 [47] E.E. Roden, M.M. Urrutia, Influence of Biogenic Fe(II) on Bacterial Crystalline
5 Fe(III) Oxide Reduction, *Geomicrobiology Journal*. 19 (2002) 209–251.
6 <https://doi.org/10.1080/01490450252864280>.
- 7 [48] S. Li, S. Chen, M. Wang, X. Lei, H. Zheng, X. Sun, L. Wang, Y. Han, Iron fractions
8 responsible for the variation of Cd bioavailability in paddy soil under variable
9 pe+pH conditions, *Chemosphere*. 251 (2020) 126355.
10 <https://doi.org/10.1016/j.chemosphere.2020.126355>.
- 11 [49] A. Drizo, Y. Comeau, C. Forget, R.P. Chapuis, Phosphorus saturation potential: a
12 parameter for estimating the longevity of constructed wetland systems, *Environ. Sci.*
13 *Technol.* 36 (2002) 4642–4648.
- 14 [50] L.I. Bowden, A.P. Jarvis, P.L. Younger, K.L. Johnson, Phosphorus Removal from
15 Waste Waters Using Basic Oxygen Steel Slag, *Environ. Sci. Technol.* 43 (2009)
16 2476–2481. <https://doi.org/10.1021/es801626d>.
- 17 [51] M. Zuo, G. Renman, J.P. Gustafsson, W. Klysubun, Phosphorus removal by slag
18 depends on its mineralogical composition: A comparative study of AOD and EAF
19 slags, *Journal of Water Process Engineering*. 25 (2018) 105–112.
20 <https://doi.org/10.1016/j.jwpe.2018.07.003>.
- 21